

Research Paper

Running titles: S. Kore-eda *et al.*
Transcriptional profiles of metabolite transporters in ice plant

Transcriptional profiles of organellar metabolite transporters during induction of Crassulacean acid metabolism in *Mesembryanthemum crystallinum*.

Key words: Crassulacean acid metabolism, salinity stress, common ice plant, metabolite transporters, transcript abundance, circadian clock

Shin Kore-eda^A, Chiyuki Noake^A, Masahisa Ohishi^A, Jun-ichi Ohnishi^A and John C. Cushman^{B,C}

^ADepartment of Biochemistry and Molecular Biology, Saitama University, Saitama City, 338-8570, Japan

^BDepartment of Biochemistry and Molecular Biology, University of Nevada, Reno, NV, 89557-0014, USA

^CCorresponding author; email: jcushman@unr.edu

Abbreviations used: ANT, adenylate transporter; CAM, Crassulacean acid metabolism; DCT, dicarboxylate transporter; DMT, drug/metabolite transporter; G6P, glucose 6-phosphate; GPT, glucose 6-phosphate/Pi translocator; GS/GOGAT cycle, glutamine synthetase/glutamate synthase cycle; mCP, mitochondrial carrier protein; ME, malic enzyme; OMT, 2-oxoglutarate/malate translocator; PEP, phosphoenolpyruvate; 3-PGA, 3-phosphoglycerate; PPDK, pyruvate, Pi dikinase; PPT, phosphoenolpyruvate/Pi translocator; PT, Pi translocator; PTL, Pi translocator-like protein; RT-PCR, reverse transcriptase-coupled PCR; TPT, triose phosphate/Pi translocator; XPT, pentose phosphate/Pi translocator.

Abstract. Metabolite transport across multiple organellar compartments is essential for the operation of Crassulacean acid metabolism (CAM). To investigate potential circadian regulation of interorganellar metabolite transport processes, we have identified eight full-length cDNAs encoding an organellar triose phosphate/Pi translocator (McTPT1), a phosphoenolpyruvate /Pi translocator (McPPT1), two glucose 6-phosphate/Pi translocators (McGPT1, 2), two plastidic Pi translocator-like proteins (McPTL1, 2), two adenylate transporters (McANT1, 2), a dicarboxylate transporter (McDCT2), and a partial cDNA encoding a second dicarboxylate transporter (McDCT1) in the model CAM plant, *Mesembryanthemum crystallinum* L. We next investigated day/night changes in steady-state transcript abundance of each of these transporters in plants performing either C₃ photosynthesis or CAM induced by salinity or water-deficit stress. We observed that the expression of both isogenes of the glucose 6-phosphate/Pi translocator (McGPT1, 2) was enhanced by CAM induction, with McGPT2 transcripts exhibiting much more pronounced diurnal changes in transcript abundance than McGPT1. Transcripts for McTPT1, McPPT1, and McDCT1 also exhibited more pronounced diurnal changes in abundance in the CAM mode relative to the C₃ mode. McGPT2 and McDCT1 transcripts exhibited sustained oscillations for at least 3 days under constant light and temperature conditions suggesting their expression is under circadian clock control. McTPT1 and McGPT2 transcripts were preferentially expressed in leaf tissues in either C₃ or CAM modes. The leaf-specific and/or circadian controlled gene expression patterns are consistent with McTPT1, McGPT2 and McDCT1 playing CAM-specific metabolite transport roles.

Introduction

Crassulacean acid metabolism (CAM) is an ecophysiological adaptation of photosynthetic carbon acquisition to limited water availability that is characterized by nocturnal CO₂ fixation into organic acids and daytime CO₂ re-assimilation by the Calvin-Benson cycle into storage carbohydrates, that generally results in improved water use efficiency (Lüttge 2004). CAM can be induced by salinity or water-deficit stress in certain plants such as *Mesembryanthemum crystallinum* L. (Cushman and Borland 2002). Transport activities that control the intracellular compartmentation and the diurnal, reciprocal fluctuations of organic acid and carbohydrates are critical to the performance of the biochemical reactions that constitute CAM. In malic enzyme (ME)-type CAM plants, such as *M. crystallinum*, nocturnal malate reserves are decarboxylated during the day in either the cytosol or mitochondria utilizing NADP-ME or NAD-ME, respectively, generating pyruvate and CO₂. The pyruvate is subsequently converted to phosphoenolpyruvate (PEP), by chloroplastic pyruvate orthophosphate (Pi) dikinase (PPDK), which serves as a substrate for gluconeogenesis and starch biosynthesis.

While recent work has focused attention on tonoplast transport activities (Lüttge *et al.* 2000; Hafke *et al.* 2003) and the discovery of two different types of vacuoles with distinct malate transport properties (Epimashko *et al.* 2004), less is known about the transport properties of other organelles. The physiological roles of chloroplasts in carbon metabolism change dramatically during the transition from C₃ photosynthesis to CAM (Cushman and Bohnert 1999). For example, the activity, protein, and mRNA abundance of PPDK, a chloroplast localized enzyme, are induced during the C₃ to CAM transition by salinity stress (Winter *et al.* 1982; Holtum and Winter 1982; Fißthaler *et al.* 1995). CAM induction in *M. crystallinum* is accompanied by substantial increases (10-20-fold) in the activities of several phosphorylytic and amylolytic starch degrading enzymes, including α and β amylases, starch phosphorylase and glucanotransferase (Paul *et al.* 1993; Häusler *et al.* 2000). The transitory starch reserve degradation activities of chloroplasts isolated from CAM-performing *M. crystallinum* were greater than those present in C₃-performing plants (Neuhaus and Schulte 1996). CAM induction also resulted in an increase in the steady-state transcript abundance for genes encoding starch phosphorylase and β -amylase with both transcripts being under circadian control (Dodd *et al.* 2003).

In accordance with such functional changes, transport activities within the chloroplast envelope in CAM-performing *M. crystallinum* differ profoundly from those in C₃-performing plants. Light-dependent pyruvate uptake was induced in chloroplasts from CAM-performing *M. crystallinum* by salinity stress (Kore-eda *et al.* 1996) and the CAM-chloroplasts have PEP transport activity (Neuhaus *et al.* 1988) to function together with PPDK during the day. Chloroplasts isolated from *M. crystallinum* in C₃ mode export mainly maltose, whereas chloroplasts from plants expressing CAM export mainly glucose 6-phosphate (G6P) (Neuhaus and Schulte 1996). Moreover, the G6P transport activities associated with active starch metabolism in CAM are induced in chloroplasts during the C₃ to CAM transition (Kore-eda and Kanai 1997). G6P transport was inhibited competitively by Pi and 3-phosphoglycerate (3-PGA) suggesting that G6P was transported by one or more plastidic Pi translocators (PTs). Recently, steady-state transcript abundance of a G6P/Pi translocator (GPT) and a PEP/Pi translocator (PPT) were shown to increase during the C₃ to CAM transition in *M. crystallinum*, whereas that of a triose phosphate/Pi translocator (TPT) remained nearly unchanged (Häusler *et al.* 2000). In CAM-induced plants, steady-state abundance of transcripts and transport activities of these three plastidic PTs varied diurnally with transcripts and transport activities peaking during the day.

These results suggest that G6P, rather than 3-phosphoglycerate or triose phosphates as in C₃ photosynthesis, is most likely the main substrate for daytime starch biosynthesis in CAM-performing *M. crystallinum* and that transport activities change in concert with the changing metabolic flux requirements of the diurnal CAM cycle (Häusler *et al.* 2000). These results are also consistent with diurnal changes in metabolite concentrations observed in *M. crystallinum* (Häusler *et al.* 2000) and other CAM species (Chen *et al.* 2002).

In order to link the unique metabolite transport requirements essential to the performance of CAM with individual transporters, we have used leaf EST collections from *M. crystallinum* (Kore-eda *et al.* 2004) as a starting point to identify and characterize full-length cDNA clones for a novel plastidic GPT (McGPT2), two novel plastidic Pi translocator-like proteins, as well as chloroplastic and mitochondrial adenylate and dicarboxylate transporters. We compared the diurnal steady-state transcript abundance changes of these genes during the C₃ to CAM transition induced by salinity stress in leaf, stem and root tissues with the three plastidic PTs reported previously (Häusler *et al.* 2000). Interestingly, all of the transporter genes encoding putative CAM-specific transport functions exhibited diurnal expression patterns, a subset of which appeared to be under circadian clock control.

Materials and methods

Gene Isolation and sequencing of RACE fragments

Expressed sequence tags (ESTs) were initially identified and sequenced for all Pi translocators, adenylate and dicarboxylate transporters as described (Kore-eda *et al.* 2004). Five prime end fragments of cDNAs for McGPT2, McPTL1, McPTL2, McDCT1, McDCT2, McANT1 and McANT2 and 3' end fragments for McGPT2 were obtained by the rapid amplification of cDNA ends (RACE) technique using primers listed in Table 1. and the SMART™ RACE cDNA Amplification Kit (BD Biosciences (Clontech), Palo Alto, CA) according to the manufacturer's instructions. Gene specific primers, ANT1-A1, DCT1-RPB2-2 and DCT2-A1, were used instead of the 5' CDS primer included in the RACE Kit to synthesize first strand cDNAs of McANT1, McDCT1 and McDCT2, respectively. The nested RACE PCR procedure described in the manufacturer's instructions was adopted to isolate all RACE fragments, except for 5' end fragments of McANT1, McANT2 and McDCT2, which were amplified without the nested RACE PCR procedure. For isolation of the 5' end of McDCT1 cDNA, DCT1-RPB2-2 and DCT1-A5 primers designed based on the McDCT1 EST sequences were used for first strand cDNA synthesis and PCR amplification of the 5' end of the McDCT1 cDNA, respectively. Because the McDCT1 cDNA fragment isolated by this first round of PCR amplification still lacked the 5' end of McDCT1 cDNA, the primers DCT1-A7 and DCT1-A8 were redesigned based on the sequence of the partial RACE fragment of McDCT1 and used for the primary and nested RACE PCR procedures, respectively. However, a McDCT1 RACE product through the second round of PCR amplification was still partial. The partial cDNA sequence of McDCT1 carried a termination codon and a poly A sequence. The RACE cDNA fragments were ligated into the plasmid pT7Blue (EMD Biosciences (Novagen), Madison, WI) and then sequenced using a BigDye™ Terminator Sequencing Kit and an ABI PRISM® 310 Genetic Analyzer or 3700 Sequence Analyzer (Applied Biosystems, Foster City, CA). Annealing temperature and numbers of cycles used above PCR reactions are summarized in Table 1.

General sequence analysis

GenBank database searching for homologous sequences was conducted using the BLAST program (Altschul *et al.* 1990). Protein sequence alignments were conducted using ClustalX (Thompson *et al.* 1997). Phylogenetic dendrograms were constructed by the neighbor-joining method using the Phylip package (Felsenstein 2004). Hydrophathy analyses of the deduced amino acid sequences for the prediction of membrane spanning domains were performed using the SOSUI (Hirokawa *et al.* 1998) and TMHMM (Krogh *et al.* 2001) programs. The TargetP (Emanuelsson *et al.* 2000) was used to predict specific intracellular locations of protein sequences.

Plant materials

For diurnal and circadian expression analyses, *Mesembryanthemum crystallinum* L. plants were grown in soil and watered daily with 0.25 x Hoagland's solution in a growth chamber on a 12 h light (28°C, 450 to 500 $\mu\text{E m}^{-2} \text{s}^{-1}$)/12 h dark (18°C) cycle. Six-week-old plants were stressed by watering with the nutrient solution containing 0.3 M NaCl (salt-stressed) or by leaving them without watering (drought-stressed) for 10 days. The leaf tissues were collected from control (well watered), salinity-stressed and drought-stressed plants every 2 h over the 24 h day/night cycle. Ten days after starting stress treatment, the plants were transferred to a chamber with continuous light (28°C) or continuous dark conditions (18°C) at the end of the dark period. Leaf

tissues were collected at midday and midnight on day 10 of the normal day/night cycles and then every 12 h for 3 days following application of continuous light or dark conditions.

For expression analyses in various tissues, except juvenile shoots, *M. crystallinum* plants were grown hydroponically with 1 x Hoagland's solution in a growth chamber on a 12 h light (27°C, 200 to 230 $\mu\text{E m}^{-2} \text{s}^{-1}$)/12 h dark (20°C) cycle. Primary leaf and root tissues were collected from 6-week-old plants, which had been well watered or stressed by adding 0.35 M NaCl (final) to the nutrient solution for 11 days. Axillary leaf and stem tissues on side shoots were collected from 12-week-old plants, which had been well watered or stressed by high salinity for 11 days. Shoots of juvenile plants were collected from well-watered, 3.5-week-old plants grown in vermiculite.

Total RNA extraction and semiquantitative RT-PCR analysis

Total RNA samples extracted by Trizol[®] (Invitrogen, Carlsbad, CA) were treated with RNase-free DNase I (Takara, Kyoto, Japan) and subjected to semiquantitative RT-PCR analysis according to Taybi and Cushman (1999) using the PCR conditions and primers summarized in Table 2. Uniform quantities of total RNA were confirmed by agarose gel electrophoresis and staining of the ribosomal RNAs using ethidium bromide. Fifty micrograms of DNase I-treated total RNA were added to 12.5 μl of the RT-PCR reaction mixture. PCR products were subjected to the agarose gel electrophoresis and stained with ethidium bromide. Digital images of their bands in the gels were analyzed using the NIH Image program (developed at the U.S. National Institutes of Health and available on the Internet at <http://rsb.info.nih.gov/nih-image/>). All RT-PCR analyses were repeated twice with similar results. Representative data are presented. PCR products were recovered from the agarose gels and ligated into a plasmid pT7Blue (EMD Biosciences (Novagen)) followed by sequencing analysis as described above. The sequences of all fragments agreed with their respective target sequences.

Malate determination

The shoot, leaf and stem tissues (ca. 0.3 g) were collected at the beginning and the end of the light period and ground in 0.8 ml of 5% perchloric acid. The homogenates were subjected to centrifugation (10,000 rpm, 10 min, 4°C). The supernatants were neutralized with ca. 0.2 ml of 5M KOH and then clarified by centrifugation (10,000 rpm, 10 min, 4°C). Malate contents of the extracts were determined enzymatically by the end-point method (Möllering 1974).

Results and discussion

Determination of full-length cDNA sequences of transporters

For the isolation of McGPT2, a leaf EST clone (GenBank accession number, AI822397, Kore-eda *et al.* 2004) that encoded a partial amino acid sequence similar to the previously reported GPT from *M. crystallinum* (McGPT1, GenBank accession number, AAF86908, Häusler *et al.* 2000) was identified. We obtained 5' and 3' ends of this transcript by the RACE technique and determined a full-length cDNA sequence of the transcript (GenBank accession number, AB190772). The cDNA sequence was 1,739 bp in length, with an open reading frame of 1,164 bp encoding a predicted precursor protein of 388 amino acid residues (McGPT2), which was within a range of 387 to 401 amino acid residues for other plant GPTs. Hydropathy analysis of the deduced amino acid sequence suggested that the predicted protein contained 7 or 8 transmembrane-spanning domains like other plastidic PTs (Kammerer *et al.* 1998; Knappe *et al.* 2003). An alignment of precursor sequences between McGPT2 and plastidic PTs from other plants including pea and spinach TPTs suggested that the processing site of McGPT2 is located at around 60 to 70 amino acid residues from the N terminus (data not shown). The predicted sequence of the mature McGPT2 protein showed a high degree of identity with the mature proteins of McGPT1 and GPTs from other plants (79 - 84%), but significantly lower identities with TPTs and PPTs from higher plants including *M. crystallinum* (36 - 39%).

In the course of database searching, we also identified several other ESTs for two proteins that were less homologous to authentic plastidic PTs but annotated as 'plastidic PT-like proteins (PTLs)'. To characterize these *M. crystallinum* PTLs, we isolated 5' RACE fragments and determined their full-length cDNA sequences. Two cDNA sequences, McPTL1 (1645 bp, GenBank accession number, AB190773) and McPTL2 (1760 bp, GenBank accession number, AB190774) contained open reading frames of 1044 bp and 918 bp, respectively. The deduced amino acid sequences of McPTL1 and McPTL2 showed high degree of identities to *Arabidopsis* proteins At4g32390 (82%) and At1g12500 (51%), respectively, and also showed weak identities with authentic plastidic PTs from higher plants (17 - 25%). Knappe *et al.* (2003) identified a variety of PT-homologous genes that belong to the drug/metabolite transporter (DMT) superfamily in the *Arabidopsis* genome (Jack *et al.* 2001). They classified them into 6 families according to their putative substrate-binding sites. We aligned 6 amino acid sequences of plastidic PTs and PTLs from *M. crystallinum* and 4 PTs from other plants together with 21 sequences of DMT superfamily proteins from *Arabidopsis* and a phylogenetic tree was constructed (Fig. 1). Plastidic PTs from higher plants (*pPT*) were well clustered into four subfamilies, TPT, PPT, GPT and pentose phosphate/Pi translocator (XPT), consistent with earlier reports (Fischer *et al.* 1997, Kammerer *et al.* 1998). McGPT2 clustered with McGPT1 on a branch containing *Arabidopsis* and pea GPTs, indicating that McGPT2 is a novel member of the GPT subfamily. Fig. 1 clearly indicated that McPTL1 and McPTL2 belonged to the families 'KD' and 'KV/A/G', respectively, with unknown function. The TMHMM program predicted that the precursors of McPTL1 and McPTL2 were highly hydrophobic proteins with 9 or 10 transmembrane domains, they had very short or almost no N-terminal hydrophilic region corresponding to a transit peptide, which usually ranged from 60 to 90 amino acid residues in authentic plastidic PTs. In addition, the program TargetP (Emanuelsson *et al.* 2000) did not predict a specific intracellular localization for them.

We also identified many ESTs encoding putative membrane proteins that were similar to adenylate transporters (ANTs) in plastids (McANT1) and mitochondria (McANT2) and dicarboxylate transporters (DCTs) in plastids (McDCT1) and mitochondria (McDCT2). We

isolated 5' and 3' RACE clones for each of these putative transporters and determined full-length cDNA sequences of them all except for McDCT1. The full-length cDNA sequences of McANT1 (GenBank accession number, AB190777) and McANT2 (GenBank accession number, AB190778) contained 2,469 and 1,683 bp and encoded predicted proteins of 622 and 388 amino acid residues, respectively, whose numbers were comparable to 569 to 623 amino acids for plastidic ANTs and 308 to 388 amino acids for mitochondrial ANTs from other higher plant species, respectively. The deduced amino acid sequence for the putative mature protein of McANT1 was highly homologous (83% amino acid identity) to the mature part of a plastidic ANT in *Arabidopsis* (At1g80300, GenBank accession number, Q39002), which has been shown to transport ATP and ADP (Möhlmann *et al.* 1998). Plastidic nucleotide transporters from higher plants also have significant similarities with algal and bacterial nucleotide transporters (Winkler and Neuhaus, 1999; Amiri *et al.* 2003; Linka *et al.* 2003). A phylogenetic tree constructed with McANT1 and 8 other plastidic nucleotide transporter sequences from higher plants and that from a red algae clearly showed that the McANT1 was clustered with nucleotide transporters from dicots (Fig 2a). The deduced amino acid sequence for the putative mature protein of McANT2 was 84% identical to a mitochondrial ANT from *Arabidopsis* (At3g08580, GenBank accession number, AAL06907) and 71% identical to *AAC2* gene product (GenBank accession number, P18239), which is a major isoform of ANT in yeast mitochondria (Kolarov *et al.* 1990).

For McDCT1 (1,701 bp, GenBank accession number, AB190775), only the partial cDNA sequence was determined through two rounds of 5' RACE PCR. The predicted partial amino acid sequence of McDCT1 contained 426 amino acid residues, which was shorter than 551 to 569 amino acid residues for plastidic DCTs from other higher plant species. Alignment between McDCT1 and other plastidic DCTs showed that this clone appears to lack 125 to 170 amino acid residues at the N terminus. The partial amino acid sequence of McDCT1 shared extremely high identity (91%) with a 2-oxoglutarate/malate translocator (OMT) from spinach (GenBank accession number, Q41364), a member of the plastidic DCT family. The plastidic DCTs of higher plants consist of two distinct groups with overlapping substrate specificities. The first group represented by OMTs transports dicarboxylates (malate, succinate, fumarate, glutarate and 2-oxoglutarate), whereas the second group represented by general dicarboxylate transporters (GDTs) or also referred to as glutamate/malate transporters, transport the amino acids glutamate and aspartate in addition to substrates transported by OMT (Flügge *et al.* 1988). OMT and GDT proteins also formed two distinct subfamilies based on their sequence similarities (Weber and Flügge 2002, Taniguchi *et al.* 2004). Therefore, the partial amino acid sequence of McDCT1 was aligned with 5 plastidic OMT sequences and 6 GDT sequences in the corresponding regions. The resulting phylogenetic tree clearly showed that McDCT1 clustered with dicot OMTs (Fig. 2b). This result suggested that McDCT1 is not a GDT, but a plastidic OMT of *M. crystallinum*.

The cDNA for McDCT2 (1,360 bp, GenBank accession number, AB190776) carried an open reading frame of 939 bp that encoded a predicted protein of 313 amino acid residues, whose number was comparable to 226 to 302 amino acids for well-characterized mitochondrial DCTs from other higher plants. The deduced protein sequences of mitochondrial transporters in *M. crystallinum*, McANT2 and McDCT2, were highly homologous to some members of the mitochondrial carrier protein (mCP) superfamily. Amino acid sequences for McANT2 and McDCT2 were aligned with those of 12 mCPs from *Arabidopsis* (Millar and Heazlewood 2003), an ANT from maize and a DCT from *Panicum miliaceum*. Phylogenetic analysis showed that McANT2 and McDCT2 were closely related to the ANT family (*ANT*) and the dicarboxylate transporter/uncoupling protein family (*DCT/UCP*), respectively (Fig. 2c). The deduced protein

sequence of McDCT2 is very similar to mitochondrial dicarboxylate/tricarboxylate transporters from *Arabidopsis* (AtDCT1 in Fig2c, 76% identity) and tobacco (GenBank accession number, CAC84546, 79% identity), which have been demonstrated to transport both dicarboxylates and tricarboxylates (Picault *et al.* 2002). However, it remains possible that McDCT2 might function as an uncoupling protein (UCP) in mitochondria, because the *DCT/UCP* family also includes AtUCP that has been suggested to be a UCP (Maia *et al.* 1998). Characterisation of additional members of this superfamily in *M. crystallinum* is needed to assign a more definitive functional prediction.

Effects of salinity and drought stresses on transcript abundance of putative transporters.

To characterize the expression patterns of the new members of PT and adenylate/dicarboxylate transporter families and compare them with those of previously characterized genes, we use semiquantitative RT-PCR to examine diurnal changes of steady-state transcript abundance in leaves from unstressed *M. crystallinum* performing C₃ photosynthesis and from salinity- and drought-stressed plants performing CAM (Fig. 3). The steady-state abundance of McTPT1 transcripts did not show apparent diurnal change in leaves from unstressed plants. After 10 days under salinity or drought conditions, the abundance of McTPT1 transcript not only declined, but also showed diurnal changes with peak expression occurring near the middle of the light period (Fig. 3a, c). In contrast, the steady-state abundance of McPPT1 transcripts increased in leaves following salinity stress treatment and showed enhanced diurnal expression that peaked during the light period, whereas expression remained at relatively low levels throughout the light period in unstressed plants (Fig. 3a,c). We observed higher activity of PEP/Pi exchange via a plastidic PPT in crude extracts from leaves of CAM-performing *M. crystallinum* than C₃-performing plants by reconstitution of membrane proteins in the extract into proteoliposomes according to Flügge and Weber (1994) (C. Noake, S. Kore-eda and J. Ohnishi, Unpublished data). Increased abundance of McPPT1 transcript in the CAM leaves may support this higher activity of PEP transport in CAM leaves.

The steady-state transcript abundance of McGPT1 increased more dramatically than that of McPPT1 following both stress treatments. However, there was a marked shift in the peak diurnal expression pattern from late dark period/early light period in C₃-performing plants to midday in CAM-performing plants that also showed elevated transcript abundance during the first half of the dark period (Fig. 3a,c). Diurnal expression patterns of McTPT1, McPPT1, and McGPT1 were similar to those reported by Häusler *et al.* (2000), although we were able to detect McPPT1 or McGPT1 transcripts in C₃-performing plants using RT-PCR, which is more sensitive in detection than the northern blotting analysis conducted in the earlier work.

In contrast to McGPT1 transcripts, McGPT2 transcripts were not detected in leaves of unstressed plants performing C₃ photosynthesis under standard PCR conditions (Table 2). Doubling total RNA input and increasing PCR cycle number from 22 to 25 permitted the detection of only trace amounts of McGPT2 transcripts in the C₃ leaves (data not shown). Under both salinity and drought stress conditions, however, GPT2 transcripts increased in abundance more strongly than McGPT1 transcripts, with maximum accumulation occurring 4 to 8 h into the light period and diminishing rapidly during the latter half of the dark period (Fig. 3a,c). Induction of G6P transport activity in chloroplast during C₃ to CAM transition (Kore-eda and Kanai 1997) may be supported by increased abundance of McGPT1 and/or McGPT2 transcripts in the CAM leaves observed here. The abrupt increase in the transcript abundance of GPTs at four hours into the light period may reflect the increased demand for G6P that is required for daytime starch

biosynthesis in plastids during Phase III of CAM (Fig. 6). Häusler *et al.* (2000) observed that in *M. crystallinum* performing CAM the total membrane fraction of leaves from the light period contained somewhat higher G6P transport activities than that of leaves from the dark. However, there remains the possibility that these two GPTs may also export G6P from chloroplasts during nocturnal carboxylation and starch degradation (Phase I; Fig. 6) because their transcripts remain abundant well into the dark period and then decline gradually. In addition, the initial rate of G6P uptake into intact chloroplasts isolated from CAM-performing *M. crystallinum* leaves was inhibited about 50% by illuminating chloroplasts, suggesting that GPT(s) are likely to be subjected to post-translational regulation by light (Kore-eda and Kanai 1997). To determine the physiological relevance of diurnal fluctuations in transcript abundance to CAM, the relative amounts and/or activities of the corresponding gene products must also be assessed.

Salinity or drought stress treatments did not significantly alter the abundance of the transcripts for the plastidic Pi translocator-like protein McPTL2, although there were slight diurnal fluctuations with two peaks occurring after 4 to 6 h in light or in darkness (Fig. 3a, c). No analysis of McPTL1 transcript expression was performed.

In leaves from unstressed *M. crystallinum*, steady-state abundance of the transcripts for the plastidic OMT (McDCT1) exhibited a diurnal expression pattern with peak abundance occurring during the late dark and early light periods. The abundance of McDCT1 transcripts was repressed under stress conditions especially in the early dark period (Fig. 3b,c). The major function of OMT in chloroplasts from C₃ plants is the import of 2-oxoglutarate from cytosol to the stroma, where it provides the carbon backbone for reassimilation of ammonia released by photorespiration as well as for the primary assimilation of ammonia (Weber and Flügge 2002; Weber *et al.* 2004). High rates of photorespiration are suspected to occur at the end of light period, when CAM plants assimilate atmospheric CO₂ with open stomata (Maxwell *et al.* 1999; Niewiadomska *et al.* 1999). The sustained expression of McDCT1 in the light under the salinity stress condition would coincide with such a role in photorespiration. In contrast, the steady-state abundance of transcripts for the mitochondrial DCT (McDCT2) exhibited only a very slight diurnal change in leaves from unstressed plants and was largely unaffected by stress treatments (Fig. 3b,c). This suggests that McDCT2 might be a housekeeping dicarboxylate transport that is required in both C₃ and CAM leaves. In contrast to the plastidic GPTs, McPPT1 and McDCT1, steady-state abundance of transcripts for both the plastidic (McANT1) and mitochondrial (McANT2) ANTs remained relatively unchanged following stress treatments and showed no significant diurnal changes (Fig. 3b,c). Such constant transcript abundance may reflect crucial roles of these proteins in ATP provision from mitochondria to the cytosol and/or chloroplasts for biosynthetic reactions and other important housekeeping functions in both C₃ and CAM leaves. Recently it has been shown that continuous ATP supply via plastidic ANTs into developing plastids and mature chloroplasts at night is required for controlled plant development in *Arabidopsis* (Reiser, *et al.* 2004).

As a positive control, the transcript abundance for *PPC1*, a CAM-specific isogene for PEP carboxylase (McPPC1) known to be induced in the C₃ to CAM transition in *M. crystallinum* (Cushman *et al.* 1989), was monitored. McPPC1 transcripts were only slightly detectable in unstressed leaves after 4 to 6 h in the light period and increased dramatically following stress treatments, confirming that CAM was induced in these plants (Fig. 3b,c). Furthermore, McPPC1 transcripts exhibited diurnal fluctuations in abundance that were lowest at the end of the dark period and at the beginning of the light period.

The *Arabidopsis* polyubiquitin gene *UBQ10* is constantly expressed in various organs

and environmental conditions (Sun and Callis 1997), over day/night cycles (Tóth *et al.* 2001) and irrespective of salinity or drought stress treatment (Boxall *et al.* 2001; 2005). A contig sequence encoding a polyubiquitin, McUBI1, homolog of *Arabidopsis* *UBQ10* was identified from several ESTs in *M. crystallinum* and was also constantly expressed in *M. crystallinum* leaves over day/night cycles and under a continuous light condition (J. Hartwell, personal communication). In this study, the steady-state abundance of McUBI1 transcripts remained relatively unchanged following stress treatments and showed no diurnal fluctuations, thus serving as a useful indicator of equal total RNA input in RT-PCR reactions (Fig. 3b,c).

Transcript abundance of putative transporters under continuous light/dark conditions.

In CAM plants, the circadian clock plays a central role in controlling many of the biochemical and physiological components to synchronize them with the CAM cycle (Borland and Taybi, 2004). Furthermore, many genes with CAM-related functions display rhythmic changes in transcript abundance controlled by the circadian clock in *M. crystallinum* (Boxall *et al.* 2001; Dodd *et al.* 2003) as are clock components themselves (Boxall *et al.* 2005). In order to investigate the possible circadian control of organelle transporter gene expression, CAM-performing *M. crystallinum* plants were grown under either continuous light or dark (and temperature) conditions and transcript abundance was tracked for 3 days at 12 h intervals. McGPT2 and McDCT1 showed continued transcript abundance fluctuations under the continuous light condition with their changes clearly sustained at least for 3 days (Fig. 4a,b). Interestingly, transcript fluctuations of McDCT1 were sustained only the first day and then declined dramatically under the continuous dark condition, whereas McGPT2 transcript declined immediately. These results suggest that different circadian clock mechanisms might control expression of these two genes. Whereas diurnal fluctuations in McPPT1 and McGPT1 were obvious, support for the circadian regulation of these transcripts is not provided by the current data and a more detailed time course is needed to clarify this possibility. McPPC1 expression is also known to be under circadian clock control (Boxall *et al.* 2001), however, this was not evident from the times at which samples were collected, but was evident in the rapid decline of its transcript abundance under continuous dark conditions. Most of other transporters, McTPT1, McPTL2, McDCT2 and McANT2, failed to exhibit apparent changes of transcript abundance under the continuous light condition and exhibited gradual decreases in transcript abundance under the continuous dark condition. On the other hand, McANT1 and McUBI1 transcript abundance was sustained for at least 3 days under both continuous conditions. Thus, an emerging consensus of expression patterns of CAM-related genes under circadian control includes sustained or dampened fluctuations under continuous light conditions and a rapid decline in transcript abundance under continuous dark conditions.

Tissue specific expression of putative transporters

Each member of plastidic PT family plays a different role according to its substrate specificity in C_3 plants. TPT exports assimilated CO_2 in the form of triose phosphates from chloroplasts to the cytosol as a precursor for sucrose synthesis in the light (Fliege *et al.* 1978; Flügge *et al.* 1989). PPT provides chloroplasts and non-green plastids with PEP from the cytosol as a substrate for the shikimate pathway (Fischer *et al.* 1997). GPT imports G6P into non-green plastids for starch synthesis and the oxidative pentose phosphate pathway (Kammerer *et al.* 1998). In accordance with their respective physiological roles, TPT and GPT are predominantly expressed in photosynthetic and heterotrophic tissues, respectively, whereas PPT appears to be present in both

types of tissues (Fischer *et al.* 1997; Kammerer *et al.* 1998). To determine if the mRNA expression of organellar transporters match their predicted physiological roles in *M. crystallinum*, we examined their tissue specific expression patterns in shoots, leaves, stems and roots in plants of different developmental stages (Fig. 5). McUBI1 displayed relatively constant transcript abundance pattern and transcripts of McPTL2, McDCT2, McANT1 and McANT2 were detected with significant abundance in all tissues tested suggesting again their housekeeping roles. In contrast, McPPC1 expression was restricted largely to salinity-stressed 6-week-old leaf tissue and unstressed and stressed 12-week-old leaf and stem tissues. PPC1 expression was also detected in root tissue consistent with earlier observations (Cushman *et al.* 1989). We also measured malate accumulation during the dark period in all tissues except roots as an indicator of CAM. Small amounts of malate accumulated during the night in 3.5-week-old shoot, 6-week-old leaf and 12-week-old stem tissues from unstressed plants (0.10, 0.59 and 0.11 $\mu\text{mol/gFW}$, respectively). In contrast, significant amounts of malate were accumulated in 6-week-old leaf and 12-week-old stem tissues from stressed plants (4.19 and 1.16 $\mu\text{mol/gFW}$, respectively) and in 12-week-old leaf tissues from both unstressed and stressed plants (5.17 and 20.7 $\mu\text{mol/gFW}$, respectively) (Fig. 5a). The expression pattern of McPPC1 was generally well correlated with the extent of nocturnal malate accumulation. Photosynthetically active green stem tissues also performed CAM, however, the degree of CAM in the stem tissues, as judged by malate accumulation, was much less than those detected in leaf tissues.

As in C_3 plants, McPPT1 and McGPT1 transcripts were detected in the juvenile shoot, adult leaf and stem tissues, and root tissues suggesting they play roles in providing substrates to both shoot chloroplasts and root plastids. McDCT1 expression was also expressed in both shoot and root tissues. In contrast, almost no McTPT1 and McGPT2 transcript expression was observed in root tissues, consistent with the proposed photosynthesis-specific roles of these transporters. These expression patterns suggest that McGPT2 appears to be dedicated to CAM in chloroplast containing tissues, whereas McGPT1 may participate in both CAM and heterotrophic metabolism in green and non-green plastid containing tissues. The stress-inducible, circadian clock-controlled, photosynthetic tissue-specific expression patterns of McGPT2 make it an excellent CAM-specific gene model for investigation of the regulatory requirements for gene expression in CAM plants.

Conclusions

We have determined full-length cDNA sequences encoding a novel plastidic G6P/Pi translocator (McGPT2), functionally unknown Pi translocator-like proteins (McPTL1 and McPTL2), plastidic and mitochondrial ANTs (McANT1 and McANT2, respectively), a mitochondrial DCT (McDCT2), and a partial cDNA encoding a plastidic DCT (McDCT1) from *M. crystallinum*. We then investigated diurnal, circadian, and tissue-specific changes of the steady-state transcript abundance of these genes in shoot, leaf and root tissues of C_3 and leaf, stem and root tissues of CAM-performing *M. crystallinum*, together with plastidic PTs reported previously (McTPT1, McPPT1 and McGPT1). The expression patterns exhibited by these organellar transporter genes fell into three partially overlapping classes. Class I genes (McPPT1, McGPT1, and McGPT2) that showed increased transcript abundance coincident with CAM induction and Class II genes (Class I plus McTPT1 and McDCT1) that exhibited diurnal fluctuations in transcript abundance whether they were induced or repressed during CAM induction. Class II gene products are likely to contribute directly to carbon flux in CAM leaves including the performance of photorespiration-related transport functions. Class III genes (McPTL2, McDCT2, McANT1,

McANT2) exhibited largely unchanged transcript abundance in leaf tissues of both C₃ and CAM-performing plants. They may serve important housekeeping functions in both C₃ and CAM leaves. The functionally unknown transporter, McPTL2, is best categorized within Class II, rather than Class III, because it was slightly induced by the stresses and it displayed slight diurnal fluctuations in transcript abundance suggesting it may contribute to CAM. Furthermore, circadian transcript abundance fluctuation of at least two (McGPT2 and McDCT1) Class II genes were sustained two or three days under continuous light conditions, but declined rapidly under the continuous dark condition like McPPC1 suggesting an emerging consensus expression patterns of CAM-related genes under circadian control.

The physiological roles of plastidic transporters on carbon metabolic pathways in mesophyll cells of CAM-performing *M. crystallinum* are illustrated in Figure 6 as suggested by their expression patterns, as well as published reports on transporter activities. Two GPTs, McGPT1 and McGPT2, are likely to contribute to enhanced starch metabolism in CAM by transporting G6P across the chloroplast envelope during daytime decarboxylation (Phase III) (Fig. 6a). Both genes also display mRNA abundance well into the dark period suggesting that both may also participate in G6P export from the plastid during nocturnal carboxylation (Phase I). Although the diurnal and circadian expression patterns of McGPT1 and McGPT2 were similar to each other, McGPT2 transcripts exhibited a much more pronounced diurnal change in transcript abundance than McGPT1, except that McGPT2 expression was not sustained during the second half of the dark period. In addition, McGPT2 transcripts were hardly detected in the root tissue, whereas McGPT1 transcripts were highly expressed in this tissue. These observations suggest a division of labor between McGPT1 and McGPT2, wherein McGPT2 is a dedicated CAM-specific isoform, whereas McGPT1 is related to both CAM and heterotrophic metabolism in non-green plastids.

McPPT1 is likely to facilitate the transport of PEP as substrate for gluconeogenesis in concert with a pyruvate transporter and plastidic PDK during Phase III. McTPT1 exports triose phosphate as a substrate for daytime (Phase III and IV) sucrose synthesis in the cytosol (Fig. 6a,b). McDCT1 is likely to provide 2-oxoglutarate to the GS/GOGAT cycle in chloroplasts as a carbon backbone for reassimilation of ammonia released by photorespiration (Phase IV) like C₃ plants (Fig. 6b). Investigations into the kinetic properties as well as the relative protein abundance and/or activities in various tissues are in progress. Such information will help confirm their proposed physiological relevance to carbon flux in CAM as suggested by the detailed mRNA abundance studies reported here.

Acknowledgments

The authors are grateful to Dr. James Hartwell (University of New York, UK) for providing the contig sequence and information about the expression properties of UBI1. We appreciate Dr Ikuo Nishida (Saitama University, Japan) for valuable and helpful discussions. We also thank Ms. Yuki Matsushima for technical support. This work was supported, in part, by funding from the Asahi Glass Foundation (to S.K.) and the National Science Foundation (IBN-0196070 and DBI-9813360) and the Nevada Agricultural Experiment Station (to J.C.C.) and is published as publication No. 050xxxxx of the University of Nevada Agricultural Experiment Station.

References

- Altschul SF, Gish W, Miller W, Meyers EW, Lipman DJ (1990) Basic Local Alignment Search Tool. *Journal of Molecular Biology* **215**, 403-410.
- Amiri H, Karlberg O, Andersson SE (2003) Deep origin of plastid/parasite ATP/ADP translocases. *Journal of Molecular Evolution* **56**, 137-150.
- Borland AM, Taybi T (2004) Synchronization of metabolic processes in plants with Crassulacean acid metabolism. *Journal of Experimental Botany* **55**, 1255-1265.
- Boxall SF, Bohnert HJ, Cushman JC, Nimmo HG, Hartwell J (2001) The circadian clock and Crassulacean acid metabolism in *Mesembryanthemum crystallinum*. Poster S-18-012. 12th International Congress on Photosynthesis. Brisbane, Australia.
- Boxall SF, Foster JM, Bohnert HJ, Cushman JC, Nimmo HG, Hartwell J (2005) Conservation and divergence of the central circadian clock in the stress-inducible Crassulacean acid metabolism ice plant. Clock operation in a Crassulacean acid metabolism halophyte reveals clock compensation against abiotic stress. *Plant Physiology*. 137, xxx-xxx.
- Chen L-S, Lin Q, Nose A (2002) A comparative study of diurnal changes in metabolite levels in the leaves of three crassulacean acid metabolism (CAM) species, *Ananas comosus*, *Kalanchoë daigremontiana* and *K. pinnata*. *Journal of Experimental Botany* **53**, 341-350.
- Cushman JC, Bohnert HJ (1989) Nucleotide sequence of the gene encoding a CAM specific isoform of phosphoenolpyruvate carboxylase from *Mesembryanthemum crystallinum*. *Nucleic Acids Research* **17**, 6745-6746.
- Cushman JC, Bohnert HJ (1999) Crassulacean acid metabolism: Molecular genetics. *Annual Review of Plant Physiology and Plant Molecular Biology* **50**, 305-332.
- Cushman JC, Borland AM (2002) Induction of crassulacean acid metabolism by water limitation. *Plant, Cell and Environment* **25**, 295-310.
- Dodd AN, Griffiths H, Taybi T, Cushman JC, Borland AM (2003) Integrating diel starch metabolism with the circadian and environmental regulation of Crassulacean acid metabolism in *Mesembryanthemum crystallinum*. *Planta* **216**, 789-797.
- Emanuelsson O, Nielsen H, Brunak S, von Heijne G (2000) Predicting subcellular localization of proteins based on their N-terminal amino acid sequence. *Journal of Molecular Biology* **300**, 1005-1016.
- Epimashko S, Meckel T, Fischer-Schliebs E, Lüttge U, Thiel G (2004) Two functionally different vacuoles for static and dynamic purposes in one plant mesophyll leaf cell. *The Plant Journal* **37**, 294-300.

- Felsenstein J (2004) PHYLIP (Phylogeny Inference Package) version 3.6. Distributed by the author. Department of Genome Sciences, University of Washington, Seattle.
- Fischer K, Kammerer B, Gutensohn M, Arbinger B, Weber A, Häusler RE, Flügge U-I (1997) A new class of plastidic phosphate translocators: a putative link between primary and secondary metabolism by the phosphoenolpyruvate/phosphate antiporter. *The Plant Cell* **9**, 453-462.
- Fißthaler B, Meyer G, Bohnert HJ, Schmitt JM (1995) Age-dependent induction of pyruvate, orthophosphate dikinase in *Mesembryanthemum crystallinum* L. *Planta* **196**, 492-500.
- Fliege R, Flügge U-I, Werden K, Heldt HW (1978) Specific transport of inorganic phosphate, 3-phosphoglycerate and triosephosphates across the inner membrane of the envelope in spinach chloroplasts. *Biochimica et Biophysica Acta* **502**, 232-247.
- Flügge U-I, Woo KC, Heldt HW (1988) Characteristics of 2-oxoglutarate and glutamate transport in spinach chloroplasts. *Planta* **174**, 534-541.
- Flügge U-I, Fischer K, Gross A, Sebald W, Lottspeich F, Eckerskorn C (1989) The triose phosphate-3-phosphoglycerate-phosphate translocator from spinach chloroplasts: nucleotide sequence of a full-length cDNA clone and import of the *in vitro* synthesized precursor protein into chloroplasts. *The EMBO Journal* **8**, 39-46.
- Flügge U-I, Weber A (1994) A rapid method for measuring organelle-specific substrate transport in homogenates from plant tissues. *Planta* **194**, 181-185.
- Hafke JB, Hafke Y, Smith JAC, Lüttge U, Thiel G (2003) Vacuolar malate uptake is mediated by an anion-selective inward rectifier. *The Plant Journal* **35**, 116-128.
- Hirokawa T, Boon-Chieng S, Mitaku S (1998) SOSUI: classification and secondary structure prediction system for membrane proteins. *Bioinformatics* **14**, 378-379.
- Häusler RE, Baur B, Scharte J, Teichmann T, Eicks M, Fischer KL, Flügge U-I, Schubert S, Weber A, Fischer K (2000) Plastidic metabolite transporters and their physiological functions in the inducible crassulacean acid metabolism plant *Mesembryanthemum crystallinum*. *The Plant Journal* **24**, 285-296.
- Holtum JAC, Winter K (1982) Activities of enzymes of carbon metabolism during the induction of crassulacean acid metabolism in *Mesembryanthemum crystallinum* L. *Planta* **155**, 8-16.
- Jack DL, Yang NM, H. Saier M (2001) The drug/metabolite transporter superfamily. *European Journal of Biochemistry* **268**, 3620-3639.
- Kammerer B, Fischer K, Hilpert B, Schubert S, Gutensohn M, Weber A, Flügge U-I (1998) Molecular characterization of a carbon transporter in plastids from heterotrophic tissues: the glucose 6-phosphate/phosphate antiporter. *The Plant Cell* **10**, 105-117.

- Knappe S, Flügge U-I, Fischer K (2003) Analysis of the plastidic phosphate translocator gene family in *Arabidopsis* and identification of new phosphate translocator-homologous transporters, classified by their putative substrate-binding site. *Plant Physiology* **131**, 1178-1190.
- Kolarov J, Kolarova N, Nelson N (1990) A third ADP/ATP translocator gene in yeast. *Journal of Biological Chemistry* **265**, 12711-12716.
- Kore-eda S, Cushman MA, Akselrod I, Bufford D, Fredrickson M, Clark E, Cushman JC (2004) Transcript profiling of salinity stress responses by large-scale expressed sequence tag analysis in *Mesembryanthemum crystallinum*. *Gene* **341**, 83-92.
- Kore-eda S, Kanai R (1997) Induction of glucose 6-phosphate transport activity in chloroplasts of *Mesembryanthemum crystallinum* by the C3-CAM transition. *Plant and Cell Physiology* **38**, 895-901.
- Kore-eda S, Yamashita T, Kanai R (1996) Induction of light dependent pyruvate transport into chloroplasts of *Mesembryanthemum crystallinum* by salt stress. *Plant and Cell Physiology* **37**, 257-262.
- Krogh A, Larsson B, von Heijne G, Sonnhammer ELL (2001) Predicting transmembrane protein topology with a hidden markov model: application to complete genomes. *Journal of Molecular Biology* **305**, 567-580.
- Linka N, Hurka H, Lang FB, Burger G, Winkler HH, Stamme C, Urbany C, Seil I, Kusch J, Neuhaus HE (2003) Phylogenetic relationships of non-mitochondrial nucleotide transport proteins in bacteria and eukaryotes. *Gene* **306**, 27-35.
- Lüttge U (2004) Ecophysiology of crassulacean acid metabolism. *Annals of Botany* **93**, 629-652.
- Lüttge U, Pfeifer T, Fischer-Schliebs E, Ratajczak R (2000) The role of vacuolar malate-transport capacity in crassulacean acid metabolism and nitrate nutrition. Higher malate-transport capacity in ice plant after crassulacean acid metabolism-induction and in tobacco under nitrate nutrition. *Plant Physiology* **124**, 1335-1347.
- Maia IG, Benedetti CE, Leite A, Turcinelli SR, Vercesi AE, Arruda P (1998) AtPUMP: an *Arabidopsis* gene encoding a plant uncoupling mitochondrial protein. *FEBS Letters* **429**, 403-406.
- Maxwell K, Borland AM, Haslam RP, Helliker BR, Roberts A, Griffiths H (1999) Modulation of rubisco activity during the diurnal phases of the Crassulacean acid metabolism plant *Kalanchoë daigremontiana*. *Plant Physiology* **121**, 849-856.
- Millar AH, Heazlewood JL (2003) Genomic and proteomic analysis of mitochondrial carrier proteins in *Arabidopsis*. *Plant Physiology* **131**, 443-453.

- Möhlmann T, Tjaden J, Schwuöppe C, Winkler HH, Kampfenkel K, Neuhaus HE (1998) Occurrence of two plastidic ATP/ADP transporters in *Arabidopsis thaliana* L. -- molecular characterization and comparative structural analysis of similar ATP/ADP translocators from plastids and *Rickettsia prowazekii*. *European Journal of Biochemistry* **252**, 353-359.
- Möllering H (1974) L-(-)-malate, Determination with malate dehydrogenase and glutamate-oxaloacetate transaminase. In 'Methods of Enzymatic Analysis'. (Ed. HU Bergmeyer) pp. 163-181. (Academic Press: New York)
- Neuhaus HE, Holtum JAM, Latzko E (1988) Transport of phosphoenolpyruvate by chloroplasts from *Mesembryanthemum crystallinum* L. exhibiting Crassulacean acid metabolism. *Plant Physiology* **87**, 64-68.
- Neuhaus HE, Schulte N (1996) Starch degradation in chloroplasts isolated from C₃ or CAM (crassulacean acid metabolism)-induced *Mesembryanthemum crystallinum* L. *Biochemical Journal* **318**, 945-953.
- Niewiadomska E, Miszalski Z, Slesak I, Ratajczak R (1999) Catalase activity during C₃-CAM transition in *Mesembryanthemum crystallinum* L. leaves. *Free Radical Research* **31**, S251-S256.
- Paul MJ, Loos K, Stitt M, Ziegler P (1993) Starch-degrading enzymes during the induction of CAM in *Mesembryanthemum crystallinum*. *Plant Cell and Environment* **16**, 531-538.
- Picault N, Palmieri L, Pisano I, Hodges M, Palmieri F (2002) Identification of a novel transporter for dicarboxylates and tricarboxylates in plant mitochondria. Bacterial expression, reconstitution, functional characterization, and tissue distribution. *The Journal of Biological Chemistry* **277**, 24204-24211.
- Reiser J, Linka N, Lemke L, Jeblick W, Neuhaus HE (2004) Molecular physiological analysis of the two plastidic ATP/ADP transporters from *Arabidopsis*. *Plant Physiology* **136**, 3524-3536.
- Sun C-W, Callis J (1997) Independent modulation of *Arabidopsis thaliana* polyubiquitin mRNAs in different organs and in response to environmental changes. *The Plant Journal* **11**, 1017-1027.
- Taniguchi Y, Nagasaki J, Kawasaki M, Miyake H, Sugiyama T, Taniguchi M (2004) Differentiation of dicarboxylate transporters in mesophyll and bundle sheath chloroplasts of maize. *Plant and Cell Physiology* **45**, 187-200.
- Taybi T, Cushman JC (1999) Signaling events leading to Crassulacean acid metabolism induction in the common ice plant. *Plant Physiology* **121**, 545-556.
- Thompson J, Gibson T, Plewniak F, Jeanmougin F, Higgins D (1997) The CLUSTAL_X windows interface: flexible strategies for multiple sequence alignment aided by quality

analysis tools. *Nucleic Acids Research* **25**, 4876-4882.

Tóth R, Kevei E, Hall A, Millar AJ, Nagy F, Kozma-Bognar L (2001) Circadian clock-regulated expression of phytochrome and cryptochrome genes in *Arabidopsis*. *Plant Physiology* **127**, 1607-1616.

Weber A, Flügge U-I (2002) Interaction of cytosolic and plastidic nitrogen metabolism in plants. *Journal of Experimental Botany* **53**, 865-874.

Weber APM, Schneiderei J, Voll LM (2004) Using mutants to probe the *in vivo* function of plastid envelope membrane metabolite transporters. *Journal of Experimental Botany* **55**, 1231-1244.

Winkler HH, Neuhaus HE (1999) Non-mitochondrial ATP transport. *Trends in Biochemical Sciences* **24**, 64-68.

Winter K, Foster JG, Edwards GE, Holtum JAM (1982) Intracellular localization of enzymes of carbon metabolism in *Mesembryanthemum crystallinum* exhibiting C₃ photosynthetic characteristics or performing Crassulacean acid metabolism. *Plant Physiology* **69**, 300-307.

Fig. 1. A phylogenetic tree of the drug/metabolite transporter (DMT) superfamily in higher plants. In addition to 4 plastidic PT and 2 PTL sequences from *M. crystallinum*, 21 DMT sequences from *Arabidopsis* and 4 plastidic PT sequences from other higher plants were aligned by ClustalX and a phylogenetic tree was constructed by the neighbor-joining method. The transporters whose substrate specificity has been demonstrated experimentally are boxed. Putative transporter families were assigned according to Knappe et al. (2003). *NST* and *pPT* represent nucleotide sugar transporter and plastid PT families, respectively. *KD*, *KT* and *KV/A/G* families are functionally unknown and named after the amino acid residues located at their putative substrate-binding site. Branch lengths correspond to 0.1 substitutions per site. Gene locus numbers of *Arabidopsis* predicted proteins used in this phylogenetic analysis include: AtGPT1, At5g54800; AtGPT2, At1g61800; AtPPT1, At5g33320; AtPPT2, At3g01550; AtTPT, At5g46110; AtXPT, At5g17630. Accession numbers of other amino acid sequences obtained from GenBank are: BoPPT, AAA84892; McGPT1, AAF86908; McPPT1, AAF86907; McTPT1, AAF86906; PsGPT, AAC08525; PsTPT, P21727; SoTPT, P11869. Abbreviations for plant names: At, *Arabidopsis thaliana*; Bo, *Brassica oleracea*; Mc, *Mesembryanthemum crystallinum*; Ps, *Pisum sativum*; So, *Spinacia oleracea*.

Fig. 2. Phylogenetic trees for adenylate and dicarboxylate transporters from *M. crystallinum* and their homologues from plants and an alga. (a) A plastidic adenylate transporter (ANT) from *M. crystallinum* (McANT1) and 9 plastidic ANTs from higher plants and a red alga, (b) a plastidic 2-oxoglutarate/malate transporter (OMT) from *M. crystallinum* (McDCT1) and 5 plastidic OMTs and 6 plastidic general dicarboxylate transporters (GDTs) from higher plants and (c) 2 putative mitochondrial transporters from *M. crystallinum* (McANT2 and McDCT2) and 14 mitochondrial carrier proteins (mCPs) from higher plants were analyzed as in Fig. 1. Functional annotations for members of mCP superfamily were adopted from Millar and Heazlewood (2003). Branch lengths correspond to 0.1 nucleotide substitutions per site. Gene locus numbers of *Arabidopsis* proteins used in this phylogenetic analysis included: AtANT1, At1g80300; AtANT2, At1g15500; AtANT3, At3g08580; AtCAC, At5g46800; AtCDC, At3g55640; AtDCT1, At5g19760; AtDCT2, At2g22500; AtDCT3, At5g01340; AtGDT1, At5g64290; AtGDT2, At5g64280; AtOMT, At5g12860; AtPiC, At5g14040; AtUCP, At3g54110. Accession numbers of other amino acid sequences obtained from GenBank were: ChANT, AAM29152; GsANT, CAC80882; OsANT1, XP_463402; OsANT2, XP_464574; PmDCT, S65042; SbGDT, AAM89394; SoGDT, CAB88250; SoOMT, Q41364; StANT, CAA71785; ZmANT, P04709; ZmGDT1, BAD06220; ZmGDT2, BAD06222; ZmOMT, BAD06219. Amino acid sequences translated locally based on TIGR (<http://www.tigr.org/tdb/tgi.shtml>) TC sequences included: HvANT, TC147916; HvOMT, TC147752; OsOMT, TC251295; SbANT, TC102891. Additional abbreviations for proteins: CAC, carnitine/acylcarnitine carrier; CDC, Ca²⁺-dependent carrier; PiC, phosphate carrier. Abbreviations for plant names: At, *Arabidopsis thaliana*; Ch, *Citrus* hybrid cultivar; Gs, *Galdieria sulphuraria*; Hv, *Hordeum vulgare*; Mc, *Mesembryanthemum crystallinum*; Os, *Oryza sativa*; Pm, *Panicum miliaceum*; Sb, *Sorghum bicolor*; So, *Spinacia oleracea*; St, *Solanum tuberosum*; Zm, *Zea mays*.

Fig. 3. Diurnal changes in transcript abundance of plastidic and mitochondrial transporters, PPC1 and UBI1 in *M. crystallinum* grown under the Light/Dark (12 h/12 h) condition. (a) Transcript abundance of plastidic PTs (McTPT1, McPPT1, McGPT1, McGPT2 and PTL2). (b) Transcript abundance of dicarboxylate transporters (McDCT1 and McDCT2), adenylate

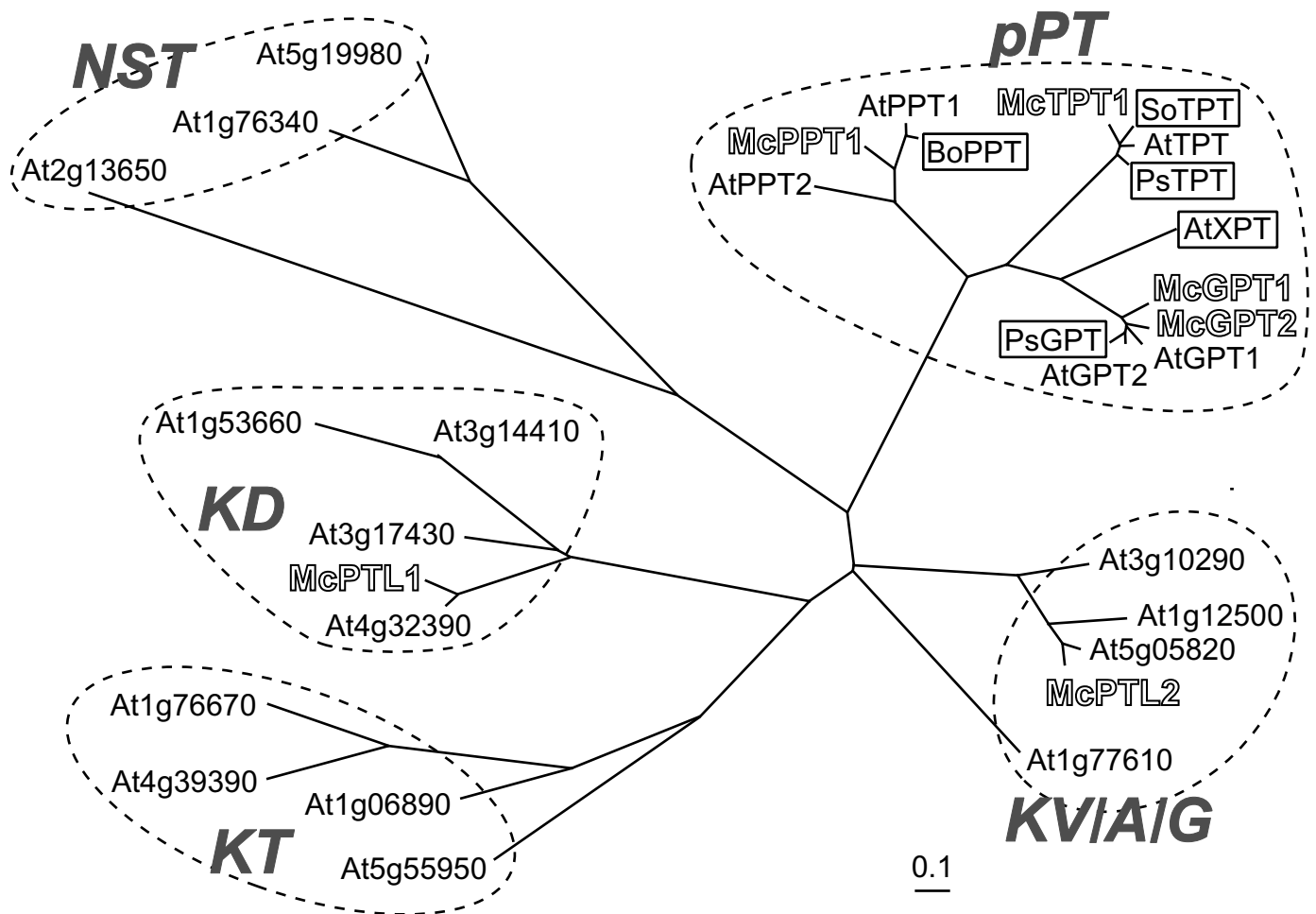
transporters (McANT1, McANT2), and a CAM-specific PEP carboxylase (PPC1) and polyubiquitin (UBI1). Leaf tissues were isolated every 2 h from *M. crystallinum* well watered (C) or stressed by high salinity (S) or by drought (D). Total RNA samples were extracted from the tissues and transcripts were detected by the semiquantitative RT-PCR method using gene specific primers. (c) Quantitative analysis of RT-PCR products from panels (a) and (b). Well watered (open circles) or stressed by high salinity (closed circles) or by drought (closed triangles). Filled and open bar represents dark and light periods, respectively.

Fig. 4. Effect of continuous light and dark and temperature conditions on transcript abundance of (a) plastidic PTs (McTPT1, McPPT1, McGPT1, McGPT2 and PTL2), (b) dicarboxylate transporters (McDCT1 and McDCT2), adenylate transporters (McANT1, McANT2), and a CAM-specific PEP carboxylase (PPC1) and polyubiquitin (UBI1). The leaves from CAM-performing *M. crystallinum* grown under the normal Light/Dark (12 h/12 h) condition were collected at 6 h after onset of light and dark periods on day 10 of salt stress treatment. Then, the plants were transferred to a continuous light (white bar) or a continuous dark (black bar) condition at the end of the dark period on day 10 and the leaves were collected every 12 h at subjective midday (L) and midnight (D) in the continuous conditions. Total RNA samples were isolated from the leaf tissues and transcripts were detected as described in Fig. 3. (c) Quantitative analysis of RT-PCR products from panel (a) under the normal Light/Dark (12 h/12 h) condition were collected at 6 h after onset of light (open circles) and dark (closed circles) periods on day 10 of salt stress treatment. Then, the plants were transferred to a continuous light (dashed lines with open triangles) or a continuous dark (dashed lines with closed triangles) condition at the end of the dark period on day 10 and the leaves were collected every 12 h at subjective midday (L) and midnight (D) in the continuous conditions. Filled and open bar represents dark and light periods, respectively.

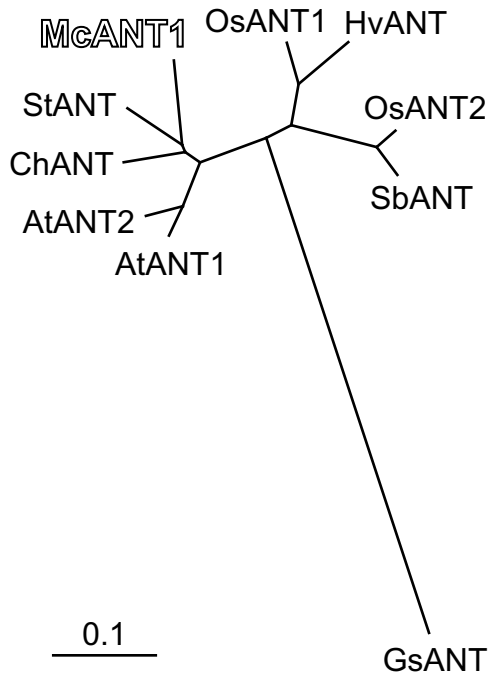
Fig. 5. Tissue-dependent expression of (a) plastidic PTs (McTPT1, McPPT1, McGPT1, McGPT2 and PTL2), dicarboxylate transporters (McDCT1 and McDCT2), adenylate transporters (McANT1, McANT2), and a CAM-specific PEP carboxylase (PPC1) and polyubiquitin (UBI1) in shoot, leaf and stem tissues in *M. crystallinum*. Shoots were collected from well watered, 3.5-week-old *M. crystallinum* grown in vermiculite. Primary leaf and root tissues were collected from 6-week-old plants grown hydroponically, which were well watered or salinity stressed for 11 days. Axillary leaf and stem tissues on side shoots were collected from 12-week-old plants grown hydroponically, which were well watered or salinity-stressed for 11 days. Total RNA samples were extracted from the tissues and transcripts were detected as described in Fig. 3. The shoot, leaf and stem tissues were collected at the beginning and the end of a light period and malate contents in the tissues were determined enzymatically. The differential malate contents measured at dawn and dusk are shown as malate accumulation during the dark period. (b) Quantitative analysis of RT-PCR products from panel (a). Filled and open bar represents dark and light periods, respectively.

Fig. 6. Plastidic carbon flux in *M. crystallinum* performing CAM. Carbon metabolisms during (a) night (Phase I) and day (Phase III) and (b) during the late afternoon (Phase IV) in a mesophyll cell of *M. crystallinum* performing CAM. Solid lines with closed arrowheads indicate photosynthetic carbon flux pathways, whereas dotted lines with open arrowheads indicate the photorespiratory pathways during Phase IV. Open and closed circles on the chloroplast envelope

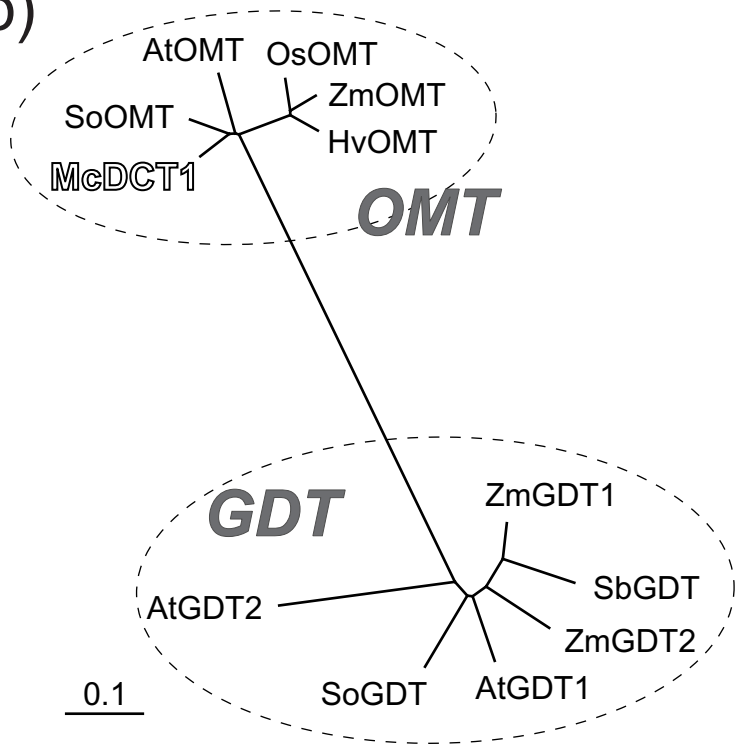
represent plastidic PTs with various substrate specificities and a McDCT1 transporter, respectively. An open diamond represents a pyruvate transporter. Additional abbreviations: GAP, glyceraldehyde 3-phosphate; NAD(P)-ME, NAD(P)-malic enzyme; OAA, oxaloacetate; 2OG, 2-oxoglutarate; Pyr, pyruvate; Triose-P, triose phosphate.



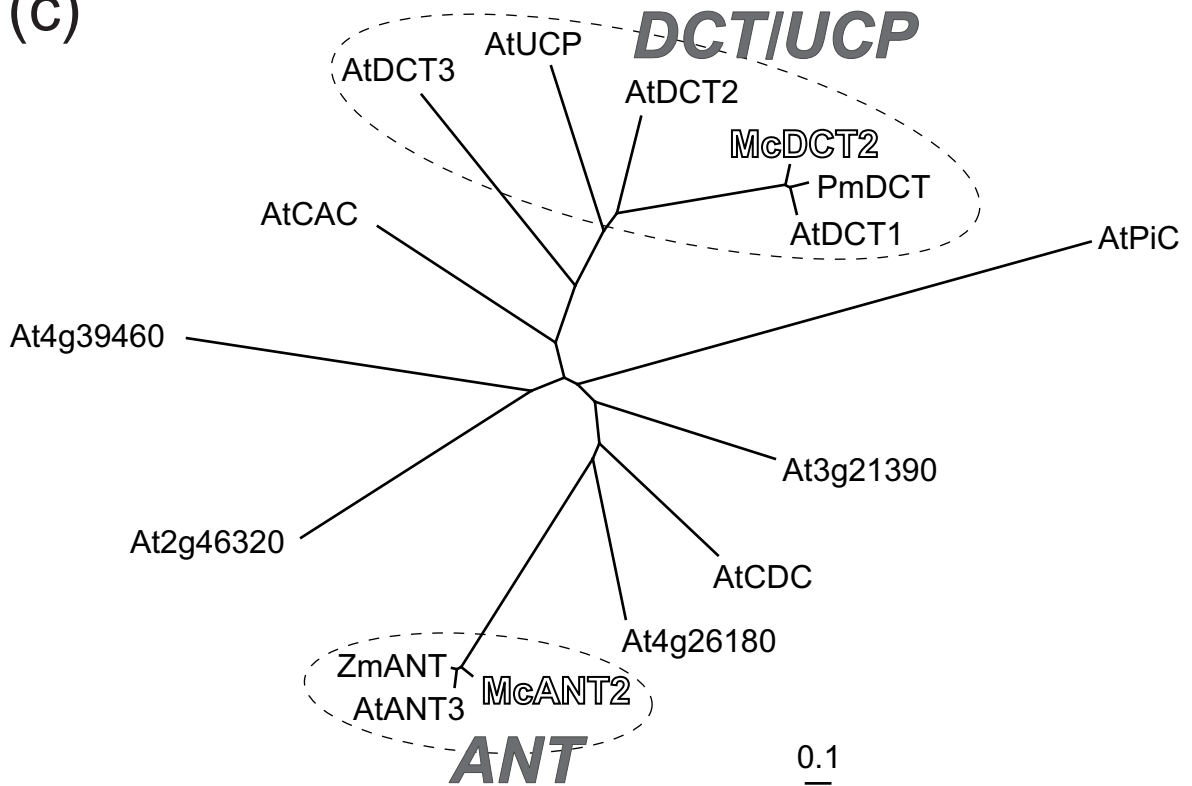
(a)

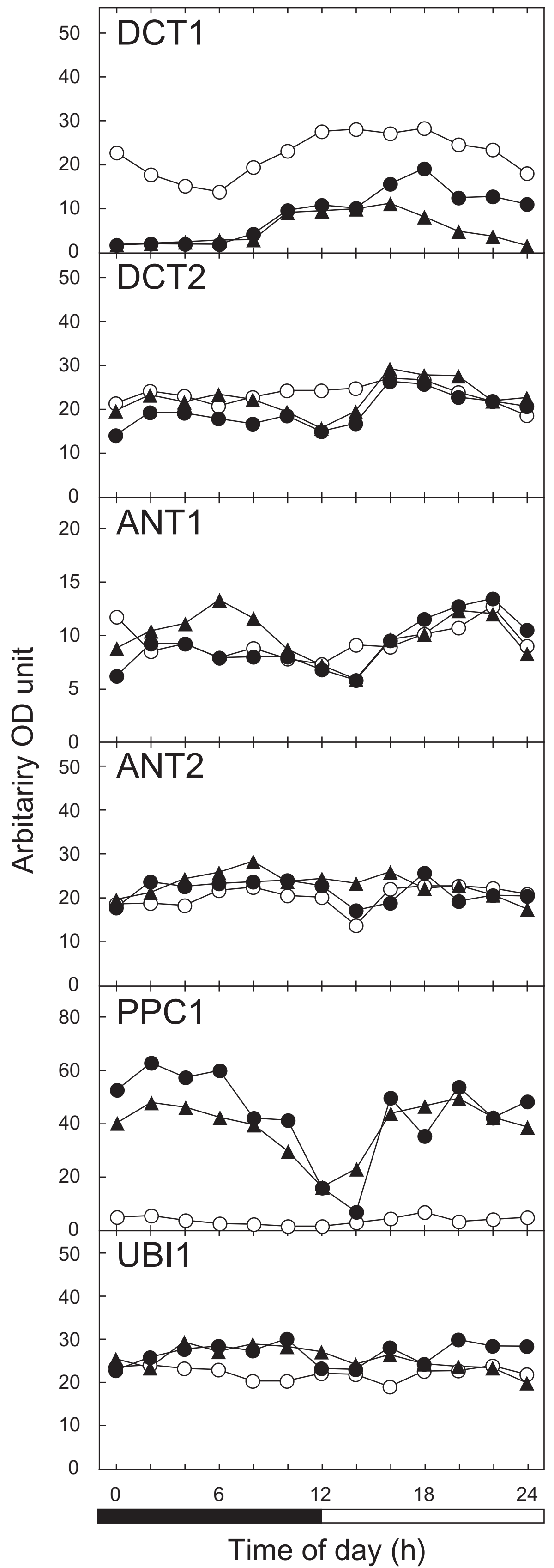
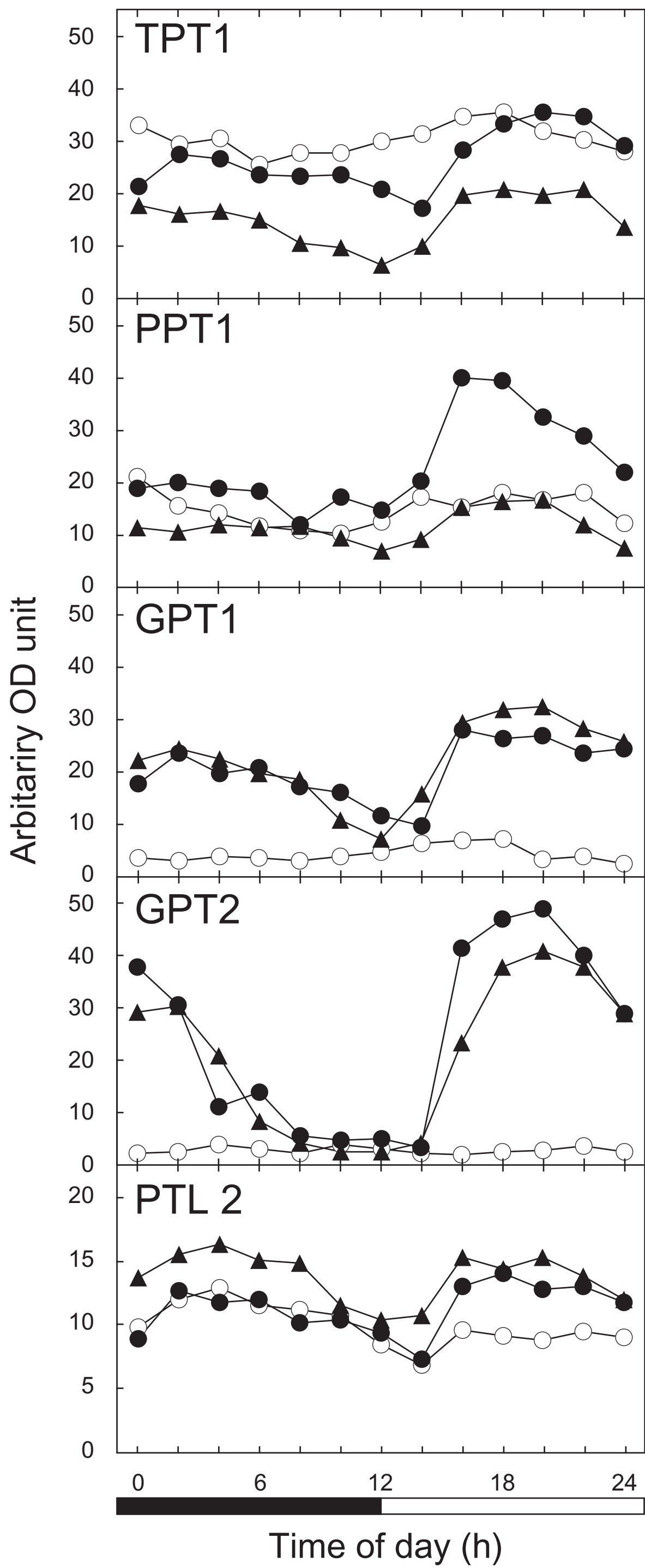


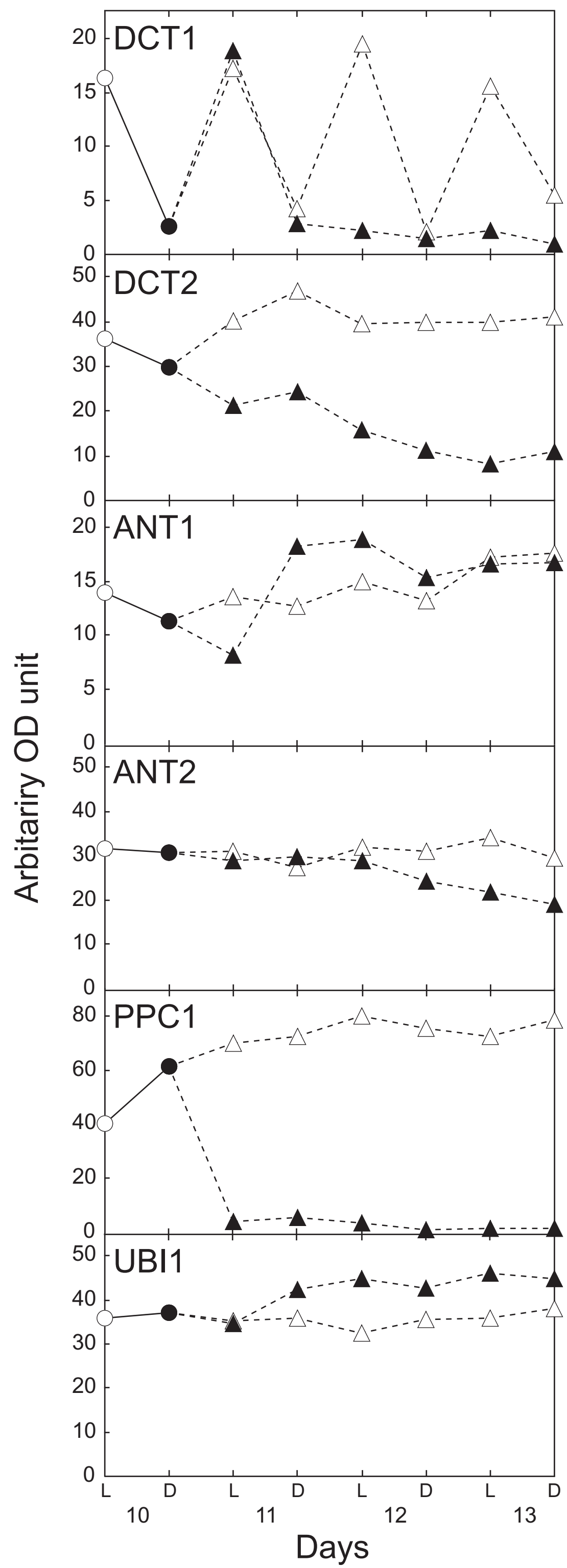
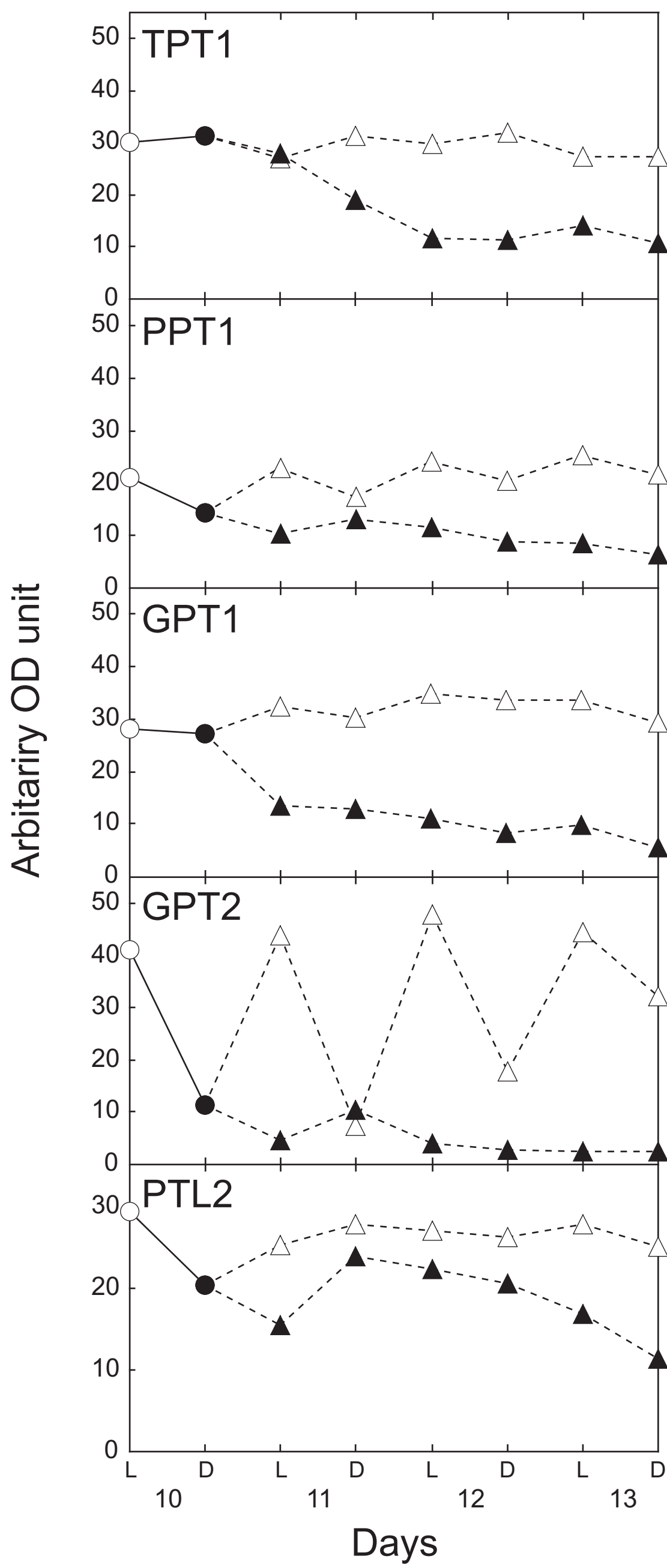
(b)

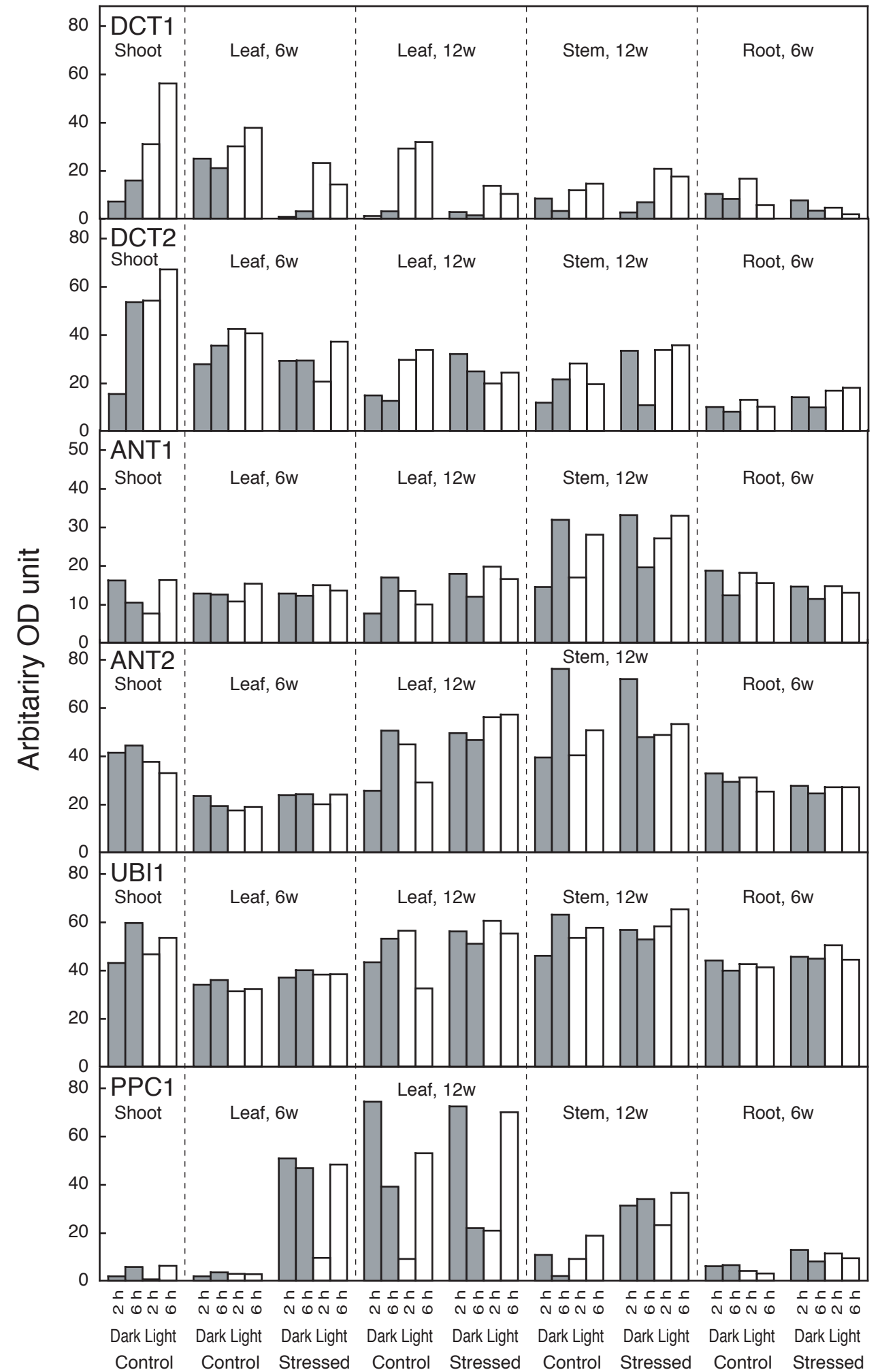
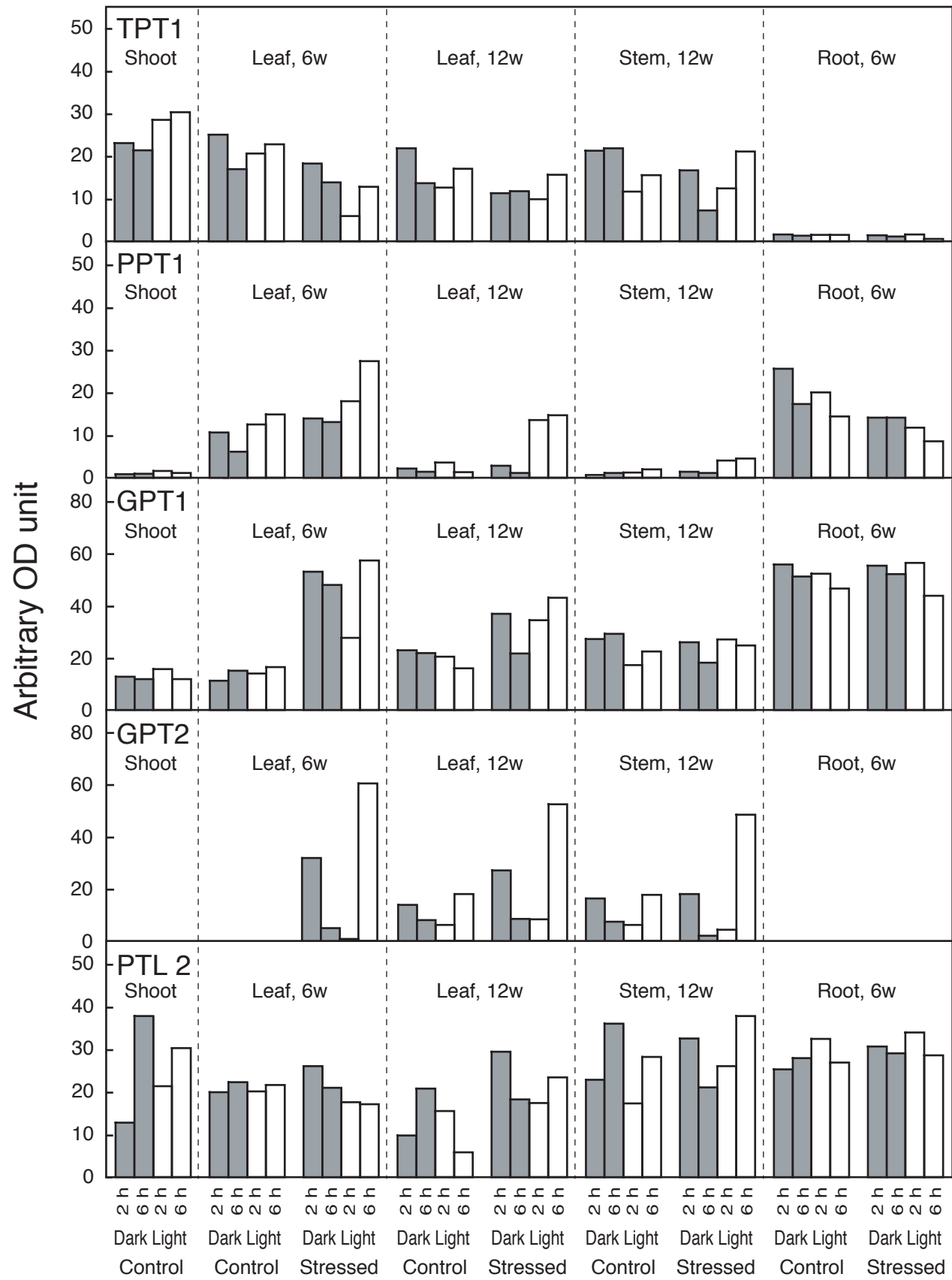


(c)









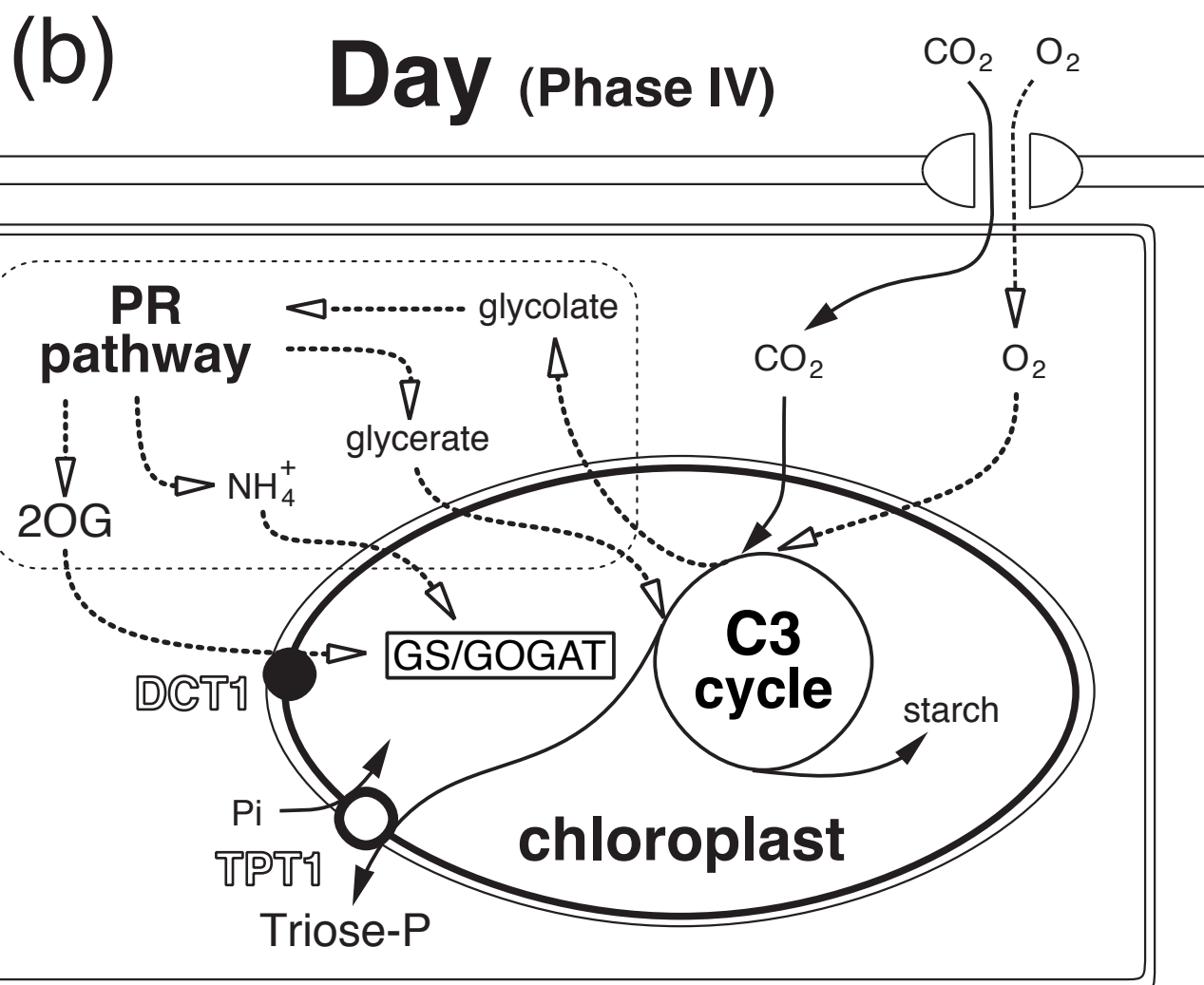
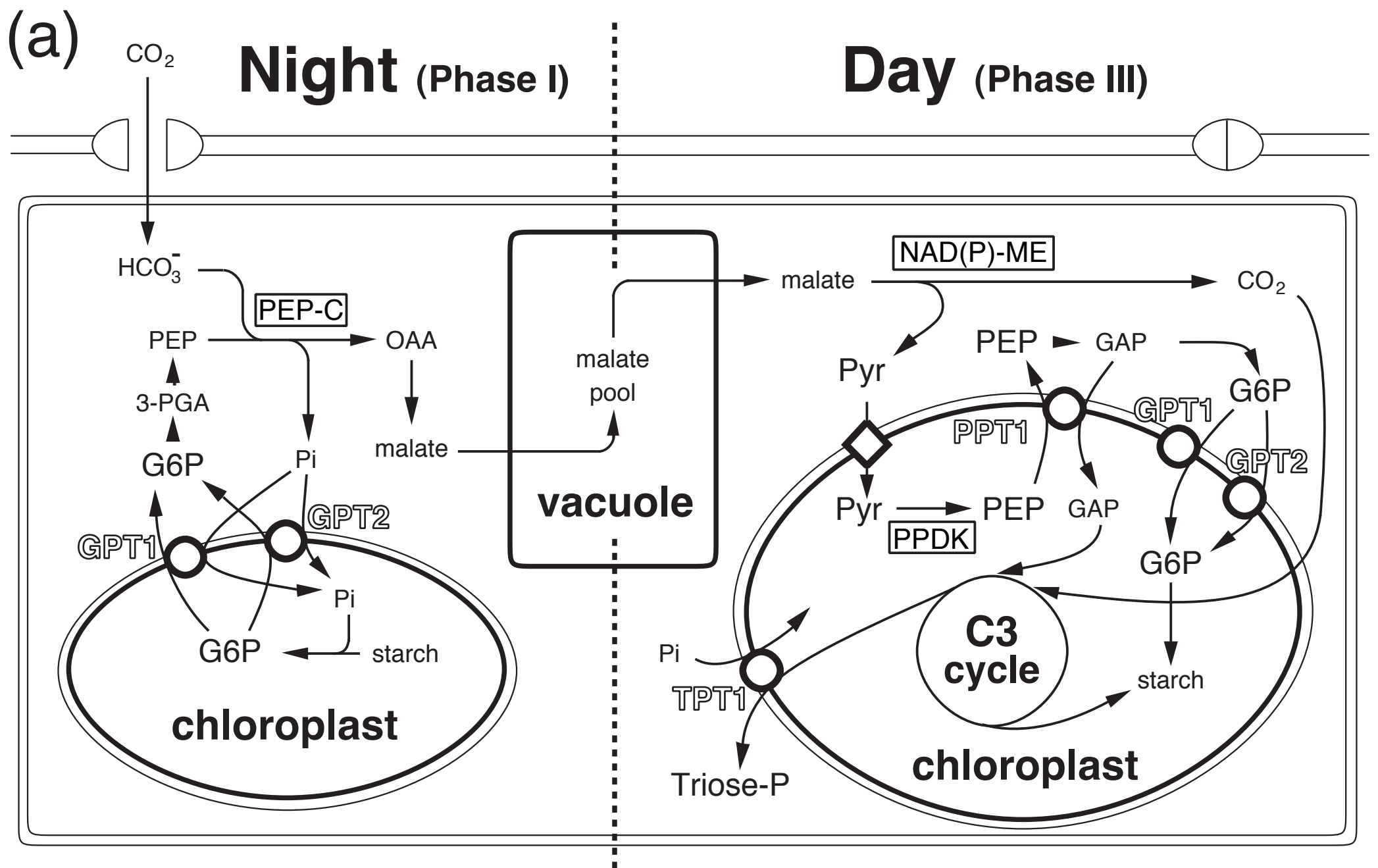


Table 1. Primer sequences and PCR conditions for isolation of 5' and 3' ends of cDNAs

Target	Type of reaction ^a	Primer		Conditions for PCR		
		Name	Sequence (5' to 3')	Annealing Temperature	Number of cycles	
McANT1	5' end	Primary RACE PCR	ANT1-A3	TCCCAGTTGCCGTAGAGAAATCACCC	62°C	35
McANT2	5' end	cDNA synthesis	ANT2-A1	GGTCAAGAGCACTGGCTTC	46°C	30
		Primary RACE PCR	ANT2-A2	ATAGCCCAGCAATACCATC		
McDCT1	5' end (1) ^b	cDNA synthesis	DCT1-RPB2-2	CAAGCAACCAAAAGTAATCAGTGGC	56°C	35
		Primary RACE PCR	DCT1-A5	GCAACTGAAAGGAAGGCTGTGAAC		
McDCT1	5' end (2) ^b	Primary RACE PCR	DCT1-A7	AAAGTGCCTCAACGGATTCGCC	72°C	30
		Nested RACE PCR	DCT1-A8	CAACCACGCCCCAAGTTTCCTCTC	68°C	30
McDCT2	5' end	cDNA synthesis	DCT2-A1	TTACAACAGTGGGAGCAG	50°C	30
		Primary RACE PCR	DCT2-A2	CCAAAGTGCCAAAACACCTTC		
McGPT2	5' end	Primary RACE PCR	GPT2-RPB	GCAAACGGTGTAAGGAGCAAC	55°C	25
		Nested RACE PCR	GPT2-A1	CACAACCACCAATGATAGG	55°C	25
McGPT2	3' end	Primary RACE PCR	GPT2-RPF	CACTGTGTAGTCTCAAGGTTTTTG	55°C	25
		Nested RACE PCR	GPT2-B1	CTATGATATCGAATGTGGC	55°C	25
McPTL1	5' end	Primary RACE PCR	PTL1-A3	ATTGTCATTCCTCCTCCCCTCAGC	63°C	35
		Nested RACE PCR	PTL1-A4	CAGACCAAGAGAAGGCAATCAAG	63°C	25
McPTL2	5' end	Primary RACE PCR	PTL2-RPB	GGATGCAATTCTACAACCTTACGC	55°C	25
		Nested RACE PCR	PTL2-A1	AGTCAAATAAAAACCGTTGCC	60°C	35

a) Primers for cDNA synthesis were used for first strand cDNA synthesis instead of the 5' CDS primer of SMART™ RACE cDNA Amplification Kit. Primers for primary RACE PCR and nested RACE PCR were used in together with the universal primer mixture and the nested universal primer of the RACE kit, respectively, to amplify respective target cDNAs by RACE PCR.

b) Primers for McDCT1 5' end (1) were designed based on McDCT1 EST sequences. Primers for McDCT1 5' end (2) were designed based on sequence of the partial 5' RACE fragment amplified by the RACE PCR procedure using primers for McDCT1 5' end (1). See **Materials and methods** for details.

Table 2. Primer sequences and PCR conditions for semiquantitative RT-PCR

Target	Forward primer		Reverse primer		Annealing Temperature	Number of cycles
	Name	Sequence (5' – 3')	Name	Sequence (5' – 3')		
ANT1	ANT1-RPF	TTAACCTTTGGGTCACCTGCC	ANT1-RPB	CTCTAAAACGATTTTCAGCATTCAG	55°C	22
ANT2	ANT2-RPF	TCGGTCTTGGTTGGCTCATCAC	ANT2-RPB	GGAAAACGTGGGGGGTTAGTC	55°C	22
DCT1	DCT1-RPF2	TACGGGTTTCGTCATCTCAGTCG	DCT1-RPB2-2	CAAGCAACCAAAGTAATCAGTGCC	55°C	22
DCT2	DCT2-RPF	TGTCTCTGGGTTCTTTGCTTCAG	DCT2-RPB	AACACTGTCCTAACTCGGTCGTCG	55°C	22
GPT1	GPT1-RPF	CGTCTCCTCCATCATCATTTTCC	GPT1-RPB	GTGCGTTGTTTCTTCCCGTG	55°C	22
GPT2	GPT2-RPF	CACTGTGTTAGTCTCAAGGTTTTTG	GPT2-RPB	GCAAACGGTGTAAGGAGCAAC	55°C	22
PTL2	PTL2-RPF	TTCTCTTACGGTCCTTGGGGTC	PTL2-RPB	GGATGCAATTCTACAACCTTACGC	53°C	24
PPC1	PPC1F-Ex9	CACTTAAACATGTCCTTGAG	PPC1R-3Ed	GAGCACACAGCAACAAAGA	50°C	20
PPT1	PPT1-RPF	GCTTCCAATGTGACAAACCAATC	PPT1-RPB	AATACAAGAAAACCTCCAGCAAGTGC	53°C	24
TPT1	TPT1-RPF	TGCCTACATTACCATCATCGCTC	TPT1-RPB	CCGAGGATTTCTTCAAGCAGC	55°C	22
UBI1	UBI1-RPF	TACTGGAAAGACTATCACCC	UBI1-RPB	ATGCCTCCCCTCAAACGA	58°C	22